

# UNM

---

## SELF-SHIELDING OF TRANSMISSION LINES

---

Noise Attenuation Through Field Containment

ECE551 PROBLEMS  
With  
Prof Christos Christodoulou

MARCH 14, 2017  
UNIVERSITY OF NEW MEXICO  
Albuquerque, NM 87131

## CONTENTS

<b>1.</b>	<b>INTRODUCTION.....</b>	<b>4</b>
<b>1.1.</b>	<b>Problem Statement.....</b>	<b>5</b>
<b>1.2.</b>	<b>Hypothesis.....</b>	<b>5</b>
<b>1.3.</b>	<b>Scope .....</b>	<b>5</b>
<b>2.</b>	<b>COMPONENT/SAMPLE DESCRIPTION.....</b>	<b>5</b>
<b>2.1.</b>	<b>Design Intent &amp; Function.....</b>	<b>5</b>
<b>2.2.</b>	<b>Design Options considered and rationale for down-selection .....</b>	<b>5</b>
2.2.1.	Fixed Impedance Dimensions .....	6
2.2.2.	Fixed Loop Area Dimensions .....	7
<b>2.3.</b>	<b>Design Drivers.....</b>	<b>8</b>
<b>2.4.</b>	<b>Materials .....</b>	<b>8</b>
<b>3.</b>	<b>PRODUCT PRODUCTION AND ASSEMBLY.....</b>	<b>11</b>
<b>3.1.</b>	<b>Process Capability.....</b>	<b>11</b>
<b>4.</b>	<b>TEST/MODEL DESCRIPTION.....</b>	<b>12</b>
<b>5.</b>	<b>TEST/MODEL PARAMITERS.....</b>	<b>12</b>
<b>5.1.</b>	<b>Model/Simulation .....</b>	<b>12</b>
5.1.1.	Objective .....	12
5.1.2.	Model.....	12
5.1.2.1.	Mesh .....	13
5.1.3.	Stimulation .....	14
5.1.3.1.	Stimulus .....	14
5.1.3.2.	Monitors/Probes.....	17
5.1.3.3.	Solver.....	18
<b>6.</b>	<b>TEST/MODEL RESULTS.....</b>	<b>19</b>
<b>6.1.</b>	<b>Simulation .....</b>	<b>19</b>
6.1.1.	Impedance .....	19
6.1.1.1.	Fixed Area.....	20
6.1.1.2.	Accuracy in question .....	20
6.1.2.	E and H field observation .....	21
6.1.3.	Gain .....	21
6.1.4.	Efficiency .....	23
<b>6.2.</b>	<b>Conclusion.....</b>	<b>24</b>
<b>7.</b>	<b>BIBLIOGRAPHY .....</b>	<b>25</b>

## FIGURES

Figure 1. Coincident Current Centroids .....	4
Figure 2. Fixed Impedance Standard Designs .....	6
Figure 3. Fixed Impedance Alternate Designs and sample N .....	7
Figure 4. Fixed Loop Area Standard Designs .....	8
Figure 5. Fixed Loop Area Alternate Designs .....	8
Figure 6. Flex section of Sample D.....	9
Figure 7. Rigid Flex section of Sample D Polar stack up .....	9
Figure 8. Model Material Properties .....	10
Figure 9. Material Properties .....	11
Figure 10. Mesh Properties .....	13
Figure 11. Model Parameters .....	14
Figure 12. Excitation Signal.....	15
Figure 13. Port Configuration.....	16
Figure 14. Additional Probes and Monitors .....	17
Figure 15. Time Domain Solver Set Up .....	18
Figure 16. TDR Traces of All Samples .....	19
Figure 17. Samples N and D E-fields at 0.5 GHz .....	21
Figure 18. Gain of All Samples .....	23
Figure 19. Radiation Efficiency in dB .....	24
Figure 20. Radiation Efficiency in Linear Magnitude .....	24

## 1. INTRODUCTION

The use of shielding to contend with noise or harmful EMI/EMR energy is not a new concept. An inevitable trade that must be made for shielding is physical space and weight. Space was often not as much of a painful design trade in older larger systems as they are in today's smaller systems. Today we are packing in an exponentially growing number of functionality within the same or smaller volumes. As systems become smaller and space within systems become more restricted, the implementation of shielding becomes more problematic. Often, space that was used to design a more mechanically robust component must be used for shielding. As the system gets smaller and space is at more of a premium, the trades starts to result in defects, designs with inadequate margin in other performance areas, and designs that are sensitive to manufacturing variability. With these challenges in mind, it would be ideal to maximize attenuation of harmful fields as they inevitably couple onto transmission lines without the use of traditional shielding. Dr. Tom Van Doren proposed a design concept for transmission lines to a class of engineers while visiting New Mexico. This design concept works by maximizing Electric field (E) and Magnetic Field (H) field containment between operating transmission lines to achieve what he called "Self-Shielding". By making the geometric centroid of the outgoing current coincident with the return current, maximum field containment is achieved. The reciprocal should be true as well, resulting in greater attenuation of incident fields. Figure's 1(a)-1(b) are examples of designs where the current centroids are coincident. Coax cables are good examples of transmission lines with co-located centroids but they demonstrate excellent field attenuation for other reasons and can't be used to test this design concept. Figure 1(b) is a flex circuit design that demonstrate the implementation of self-shielding vs a standard conductor layout seen in Figure 1(c) (Doren 20).

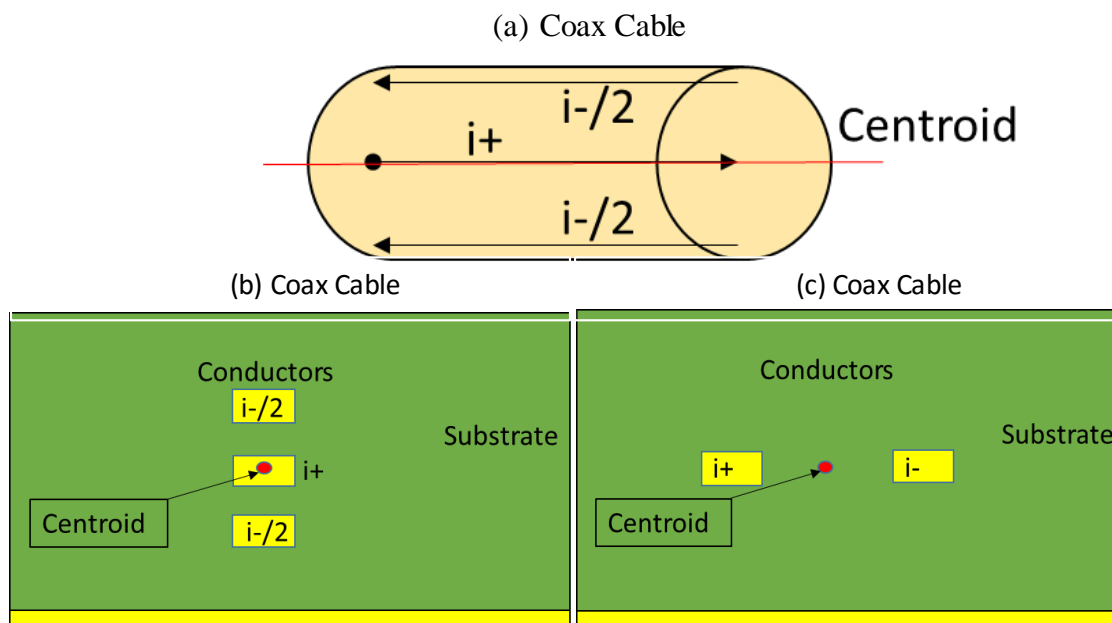


Figure 1. Coincident Current Centroids

### **1.1. Problem Statement**

Noise errors always requires a noise source, a coupling mechanism and a component sensitive to noise (Doren 8) (Ott 18). Disable or remove one of these three components of noise and you eliminate the noise error. Transmission lines can be noise source's and coupling mechanisms for noise in that they can operate as antennas. They can operate as receiving antenna's (coupling mechanisms) delivering energy to other components. They can operate as transmitting antenna (noise source's) transmitting noise. Designing out a transmission lines tendency to emit and/or receive noise through field containment is the focus of this project.

### **1.2. Hypothesis**

Field containment is enhanced and its performance as a noise source or receiver is reduced when the centroid of outgoing and returning current is co-located.

### **1.3. Scope**

In addition to testing this Hypothesis, a method for modeling transmission lines as antenna's will be developed using CST. The two modeling methods will allow a designer to characterize the transmission line as a transmitting antenna and as a receiving antenna using CST. The Hypothesis will be tested by modeling flex circuit designs with self-shielding and without self-shielding. The parameters used as a metric for differentiating the design's performance will be common antenna parameters. The Gain and Antenna Radiation Efficiency will be the most important parameters. Effective height will be measured on one design to demonstrate a method for characterizing the transition line as a receiving antenna. Impedance and loop area of the traces will be used as constraints. Loop area is the area between the traces carrying a signal. The length, materials, and width of the ground plane will be fixed for all of the samples.

## **2. COMPONENT/SAMPLE DESCRIPTION**

### **2.1. Design Intent & Function**

This project serves as an accelerated learning cycle that could feed into many future custom designs. These layouts could be utilized in high frequency applications and in low frequency application. This means that impedance will need to be controlled in some applications but not in others. As a result, Impedance can be a constraint in future applications.

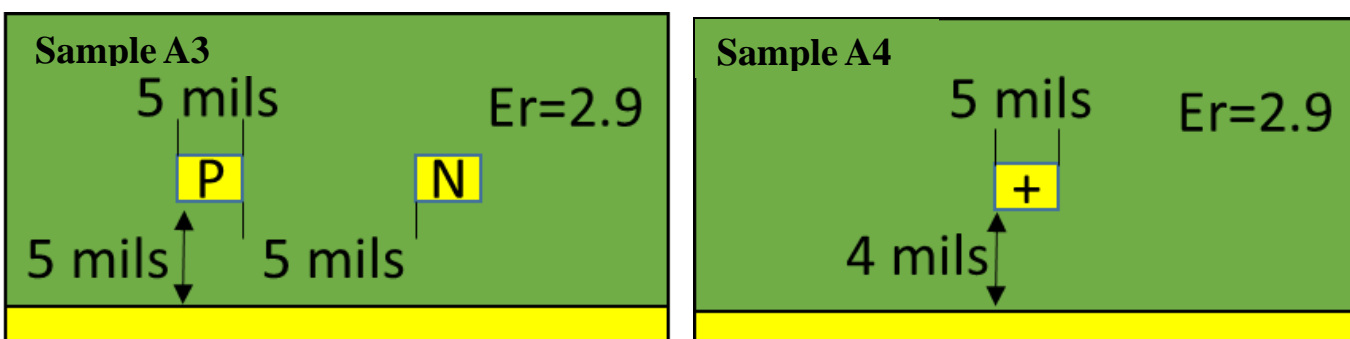
### **2.2. Design Options considered and rationale for down-selection**

Unfortunately, when a specific impedance must be maintained it forces the designer to spread out the traces. The self-shielded design works because they achieve strong field coupling between traces. This tight field coupling produces lower impedance. Unfortunately, spreading out the traces is counterproductive in testing the stated hypothesis. For this reason, the Designs will be split onto two groups. One group will be evaluated allowing loop area or trace spacing to change so that 100 Ohms differential impedance can be maintained for the differential designs and 50 Ohms impedance for single ended designs. The second set will simply fix the loop area for all designs. The fixed loop area will be 120,000 mils for all 12-inch cable. There are three

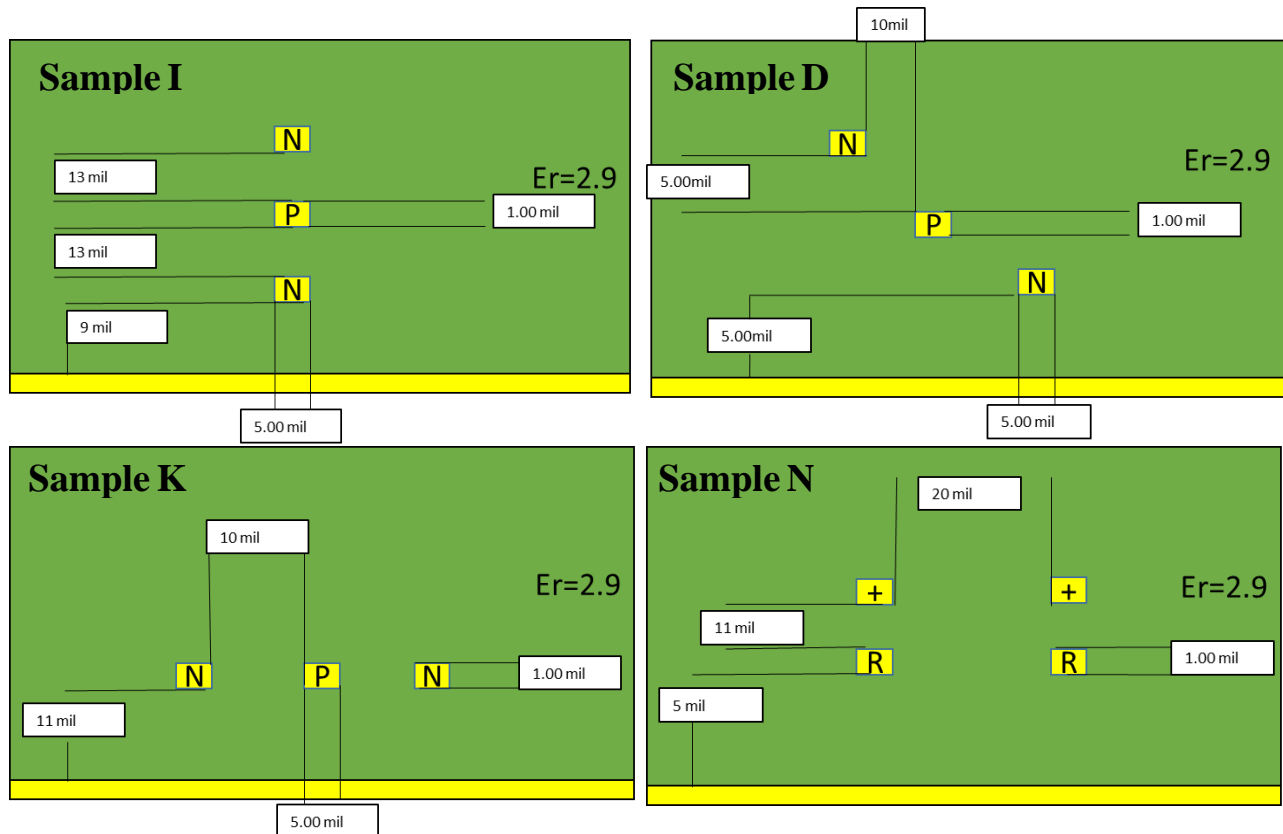
standard designs and three self-shielded designs. The standard designs include samples A3, A4 and sample N. The self-shielded designs include samples I, D, K.

### 2.2.1. Fixed Impedance Dimensions

The impedance constraint is a difficult constraint to implement as a practical design option using spacing that doesn't completely negate our attempts to test the stated hypothesis. Small trace widths and the lowest possible dielectric constant was used for all designs in order to maintain the closest spacing possible under the constraint of controlled impedance. The lowest possible dielectric constant that could be achieved with available materials was 2.9. Decreasing trace surface area would decrease coupling between traces. The smallest trace widths that could be reliably used is 5 mils. Figures 2 and 3 illustrate the smallest dimensions that could be used while maintaining a differential impedance of 100 Ohms plus or minus 10 ohms.



**Figure 2. Fixed Impedance Standard Designs**



**Figure 3. Fixed Impedance Alternate Designs and sample N**

### 2.2.2. Fixed Loop Area Dimensions

The loop area was fixed in the designs illustrated in figures 4 and 5. Figures 2 through 6 are cross section views of the flex circuit designs. The length of the designs will be fixed at 12,000 mils. Fixing the loop area to ten mils and the length to 12,000 mils will set the loop area to 120,000 mils.

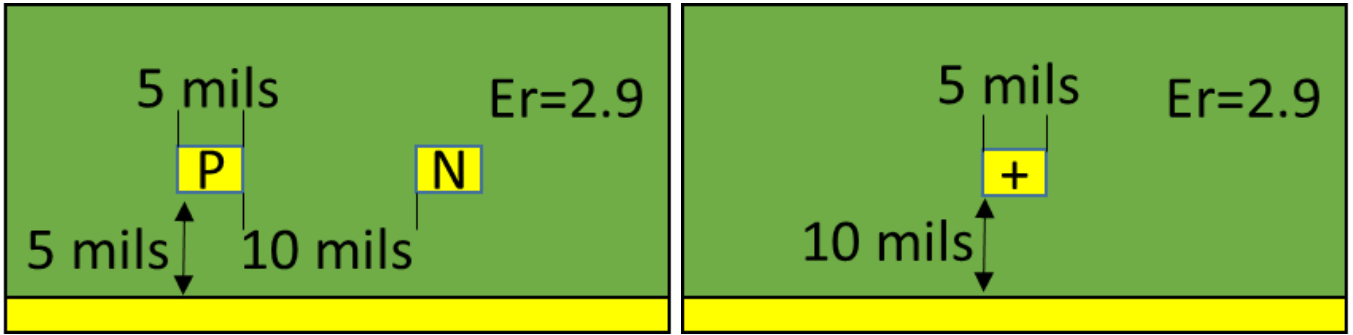


Figure 4. Fixed Loop Area Standard Designs

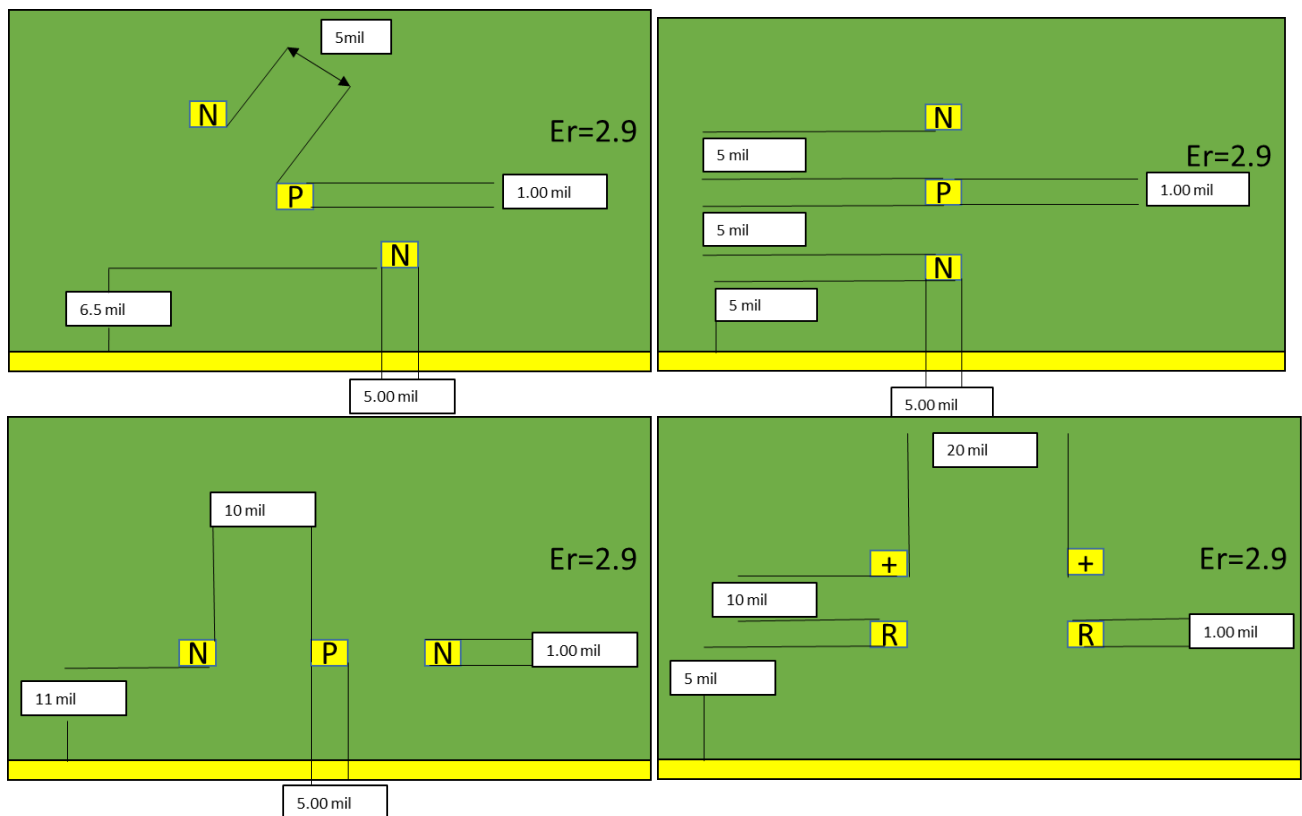


Figure 5. Fixed Loop Area Alternate Designs


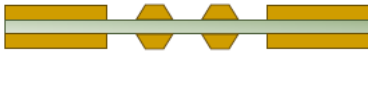
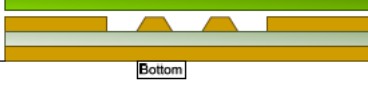
### 2.3. Design Drivers

### 2.4. Materials

The materials for the flexible portion of the sample is shown in Figure 6. The traces will be copper. The material between the traces will be AP9131 copper clad and LF0222 LF Bondply.


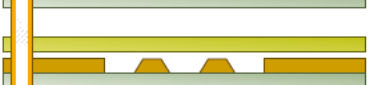
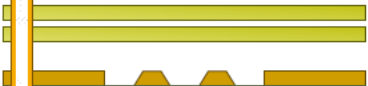





The non-copper materials between the traces maintain a dielectric constant of 2.9. The cable samples are rigid flex where the connectors are installed to provide protection during soldering and handling. The Rigid flex section of the cable includes GIA - 671N POLYIMIDE which has a dielectric constant of 3.94. The necessity to use a stiffer material and higher dielectric constant in the rigid flex portion will result in a drop in impedance in that small section of the cable. The Rigid flex will not be modeled in CST.

Layer	Stack up	Supplier Description	Stock Number	Description	Type	$\epsilon_r$	Base Thickness	Processed Thickness	File
<b>Top</b>									
2		AP9131	AP9131	1/3/1	AP COPPER CLAD	2.900	1.400	1.400	
0		LF0222	LF	BP 2/2/2	LF BONDPLY	2.900	3.000	3.000	
							1.400	1.400	
3		AP9151	AP9151	1/5/1	AP COPPER CLAD	2.900	1.400	1.400	
4							5.000	5.000	
							1.400	1.400	
5		LF0222	LF	BP 2/2/2	LF BONDPLY	2.900	5.000	5.000	
6		AP9151	AP9151	1/5/1	AP COPPER CLAD	2.900	1.400	1.400	
							5.000	5.000	
	<b>Bottom</b>						1.400	1.400	

Notes: Copper Thickness = 8.400 | Dielectric Thickness = 23.000 | Solder Mask Thickness = 0.000 | Stack Up Thickness = 31.400

**Figure 6. Flex section of Sample D**

Layer	Stack up	Supplier Description	Stock Number	Description	Type	$\epsilon_r$	Base Thickness	Processed Thickness	File
<b>Top</b>									
1		SOLDER MASK		SOLDER MASK	SODERMASK	4.000			
		IPC-MF-150	H OZ. FOIL + PLATING	Copper Foil	Copper		2.100	3.300	
		GIA - 671N	2 PLIES	PGIJ 1080 NF	POLYIMIDE B - STAGE	3.940	5.000	4.953	
2		GIA - 671N	1 PLY	PGIJ 1080 NF	POLYIMIDE B - STAGE	3.940	2.500	2.477	
		AP9131	AP9131	1/3/1	AP COPPER CLAD	2.900	1.400	1.400	
							3.000	3.000	
3		GIA - 671N	1 PLY	PGIJ 1080 NF	POLYIMIDE B - STAGE	3.940	2.500	2.290	
		AP9151	AP9151	1/5/1	AP COPPER CLAD	2.900	1.400	1.400	
							5.000	5.000	
4		GIA - 671N	1 PLY	PGIJ 1080 NF	POLYIMIDE B - STAGE	3.940	2.500	2.290	
		GIA - 671N	1 PLY	PGIJ 1080 NF	POLYIMIDE B - STAGE	3.940	2.500	2.290	
							1.400	1.400	
5		AP9151	AP9151	1/5/1	AP COPPER CLAD	2.900	1.400	1.400	
							5.000	5.000	
							1.400	1.400	
6		GIA - 671N	1 PLY	PGIJ 1080 NF	POLYIMIDE B - STAGE	3.940	2.500	2.477	
		GIA - 671N	2 PLIES	PGIJ 1080 NF	POLYIMIDE B - STAGE	3.940	5.000	4.953	
		IPC-MF-150	H OZ. FOIL + PLATING	Copper Foil	Copper		2.100	3.300	
7	<b>Bottom</b>	SOLDER MASK		SOLDER MASK	SODERMASK	4.000			

Notes: Copper Thickness = 13.600 | Dielectric Thickness = 34.730 | Solder Mask Thickness = 1.400 | Stack Up Thickness = 48.330

**Figure 7. Rigid Flex section of Sample D Polar stack up**

As you can see the thicknesses of the POLYIMIDE will change somewhat during processing. The layers that are compressed implies variability in the thickness of those layers and consequently some variability in the impedance. This variability will not be modeled in CST. Figure 8 and 9 illustrate the material parameters used in CST to model the materials shown in the polar stack ups (Figure 6 & 7). The copper material was loaded from the CST material library. The copper has an electric conductivity of  $5.8e+007$  S/m and a density of  $8930$  kg/m<sup>3</sup>. The substrate materials were imported from CAD and renamed to "SUBSTRATE". The substrate was modeled with a dielectric constant of 2.9 and a tangent delta of 0.02 at 0 GHz.

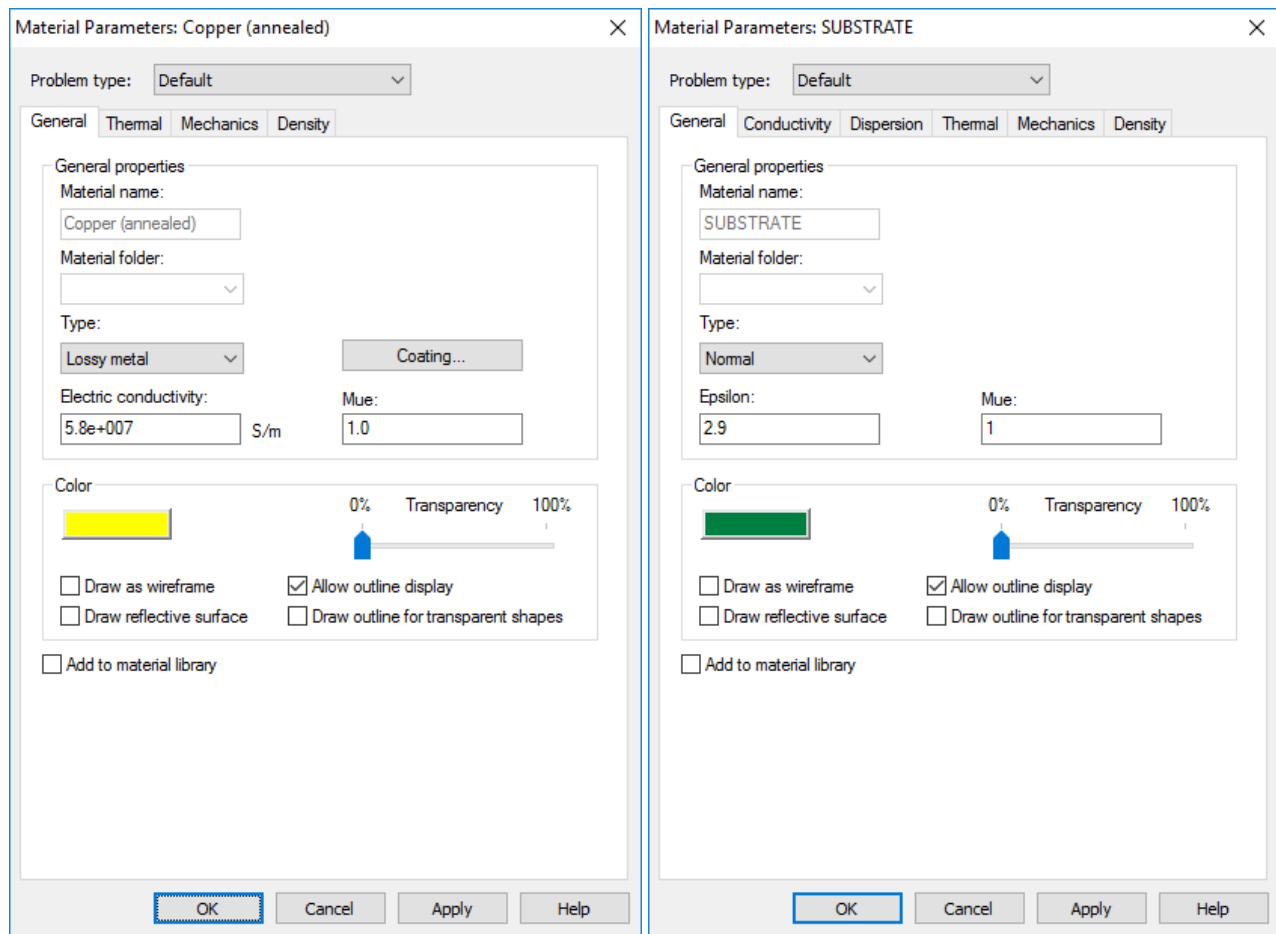


Figure 8. Model Material Properties

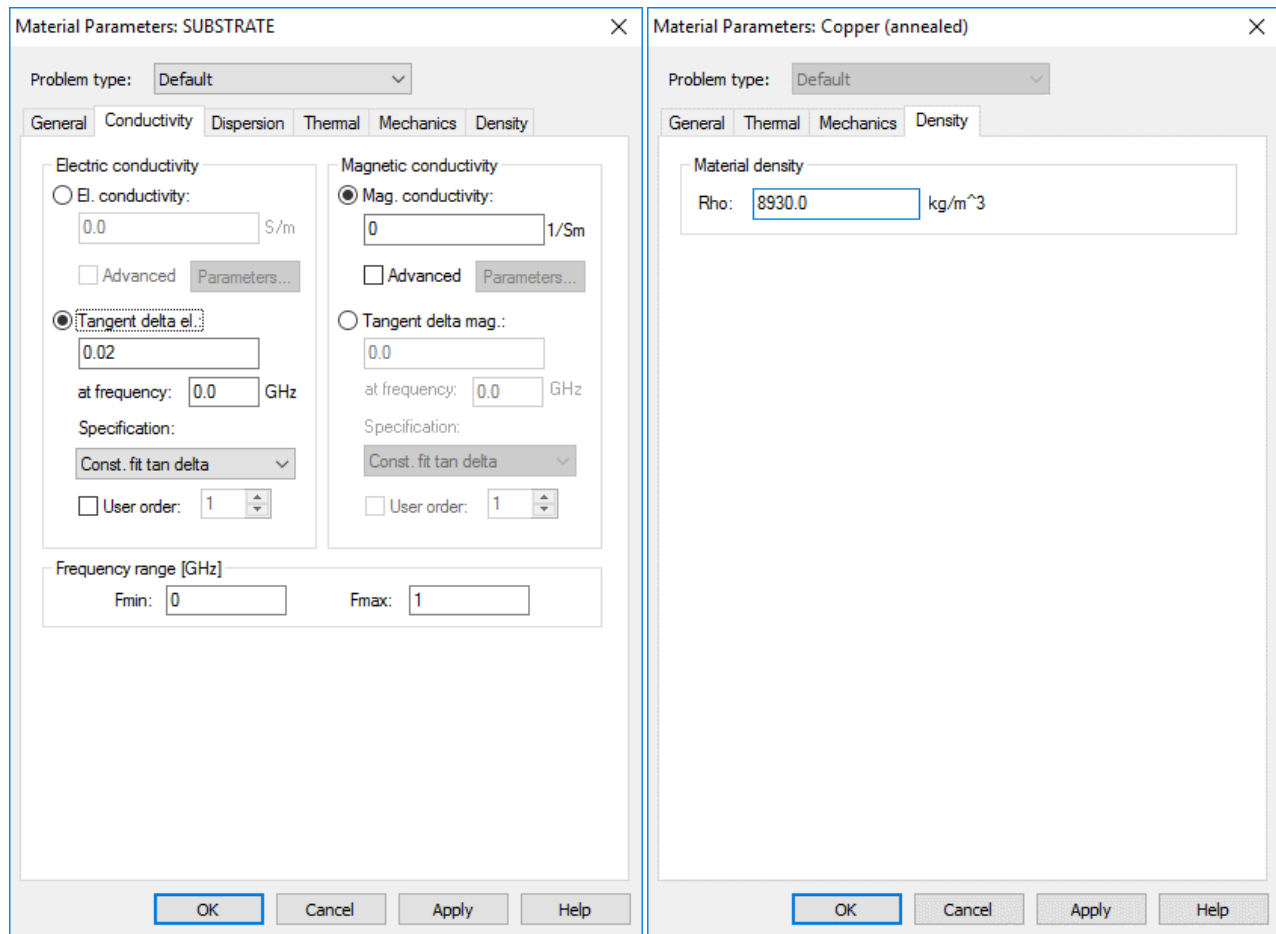


Figure 9. Material Properties

### 3. PRODUCT PRODUCTION AND ASSEMBLY

#### 3.1. Process Capability

A practical design is a design that is manufacture able. The expectation that the design be manufacture able is the driver behind the 5 mil traces and the materials discussed in earlier sections. It's important to acknowledge the discontinuities that will occur when connectorising these flex circuits. The odds are that these flex circuits will be terminated using unbalance connectors. In this case the samples will be terminated with SMA connectors which are inherently unbalance. Baluns are required to mitigate the use of unbalanced connectors. Unfortunately, baluns will not be used and it is not feasible to measure only the flexible sections of the samples. The termination of these samples will have an impact on the antenna parameters at those terminations and will drive a variance between the output of the simulation and the measurements. The model negates the termination method for two reasons. One reason is that the termination method is not necessary for testing the hypothesis. The other reason is to simplify the

model as much as possible while providing a valid and useful results. As such, only the flex portion of the samples were modeled.

## 4. TEST/MODEL DESCRIPTION

The simulation will characterize the samples transmitting performance. Gain and radiation efficiency will be used as the primary metrics for evaluating sample performance and transmitting antennas in a frequency range from 0 to 1 GHz. Only one sample will be used to simulating performance as a receiving antenna because of constrained schedule and scope.

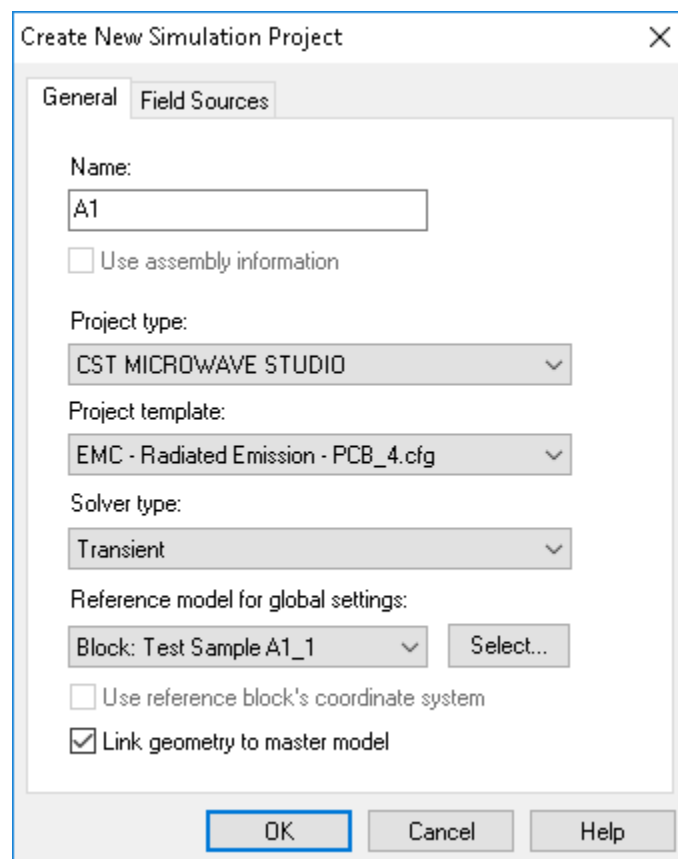
## 5. TEST/MODEL PARAMETERS

### 5.1. Model/Simulation

#### 5.1.1. Objective

#### 5.1.2. Model

The models are built using the CST Microwave Studio project type and the Electromagnetic Compatibility (EMC) radiated emissions template.



### 5.1.2.1. Mesh

The mesh parameters were selected from CST best practices communicated through CST workflows and CST technical support. The most important mesh properties used was the local mesh properties. By highlighting the copper material and instituting a specified number of 2 cells in the delta x, delta y, and delta z direction an efficient mesh was achieved. The number of cells in the length wise direction (delta y) was overridden by the global properties because these properties were more constraining. The total mesh sells were around 300,000 cells for all of the designs (See figure 10).

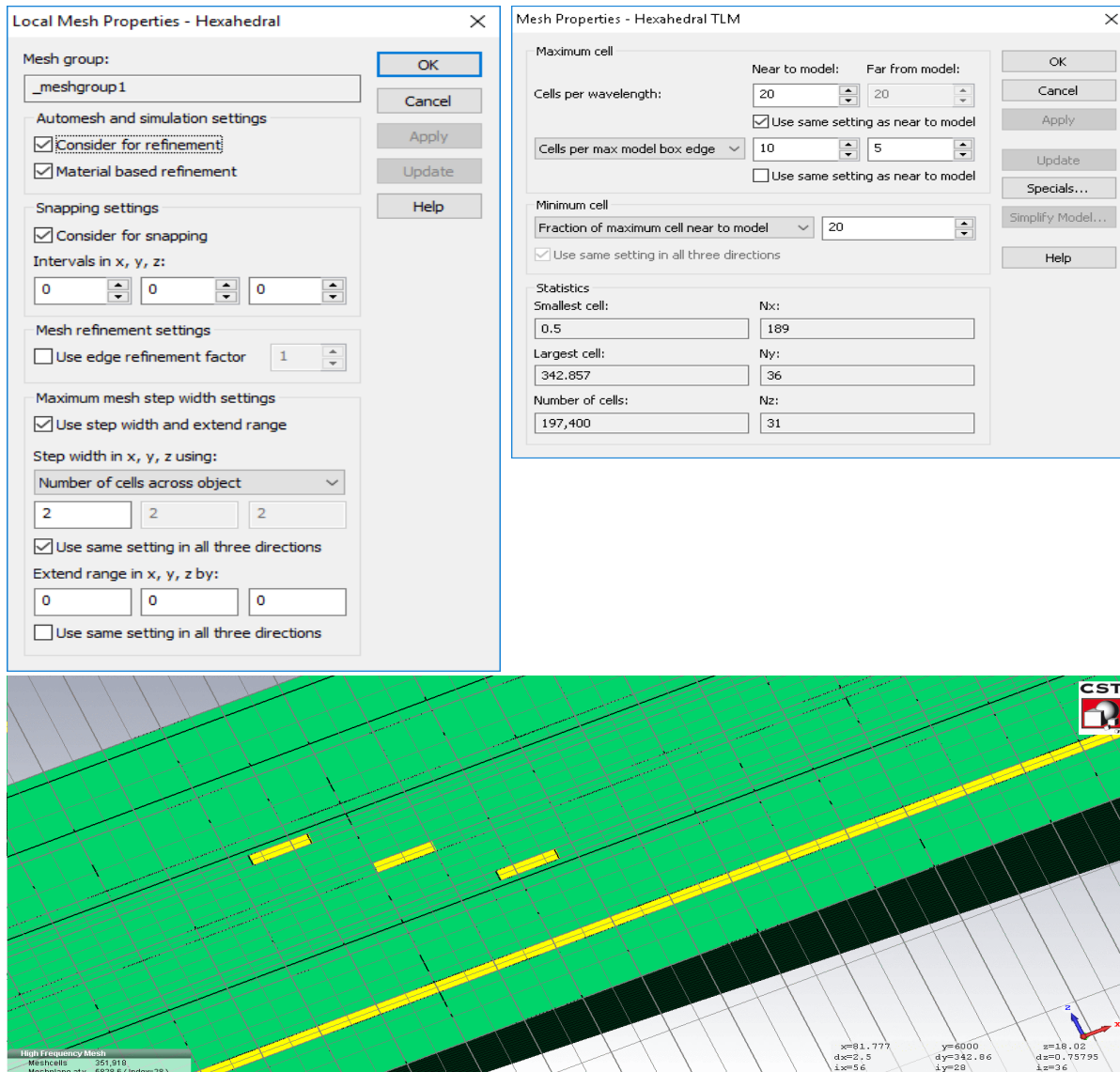
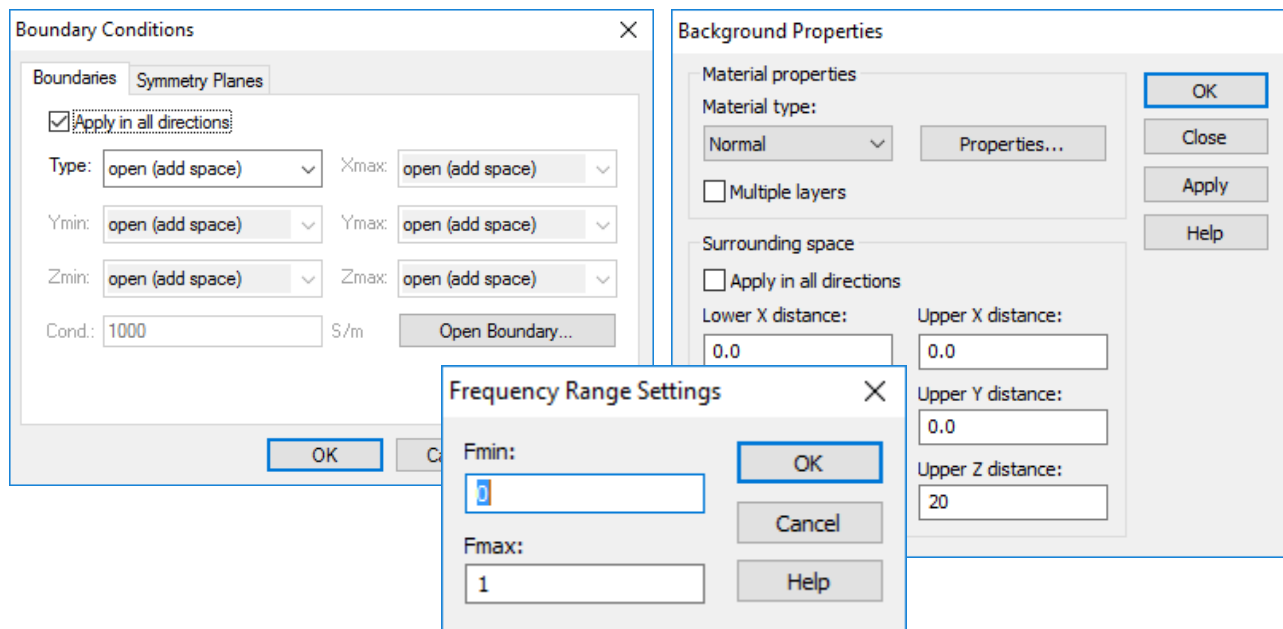


Figure 10. Mesh Properties

### 5.1.3. Stimulation

The most important frequency range to consider is the operating frequency of the transmission line. I expect digital signals will be the most common signal used on these traces. This means that the range should start at zero and not exceed 1 GHz. One GHz is chosen as the upper operating range in order to be conservative. It is noted that frequencies outside of the systems operating range should be considered when designing for EMC compatibility since noise sources may come from any frequency range. None the less, the frequency range for this study was selected to be between 0 and 1 GHz for efficiency.



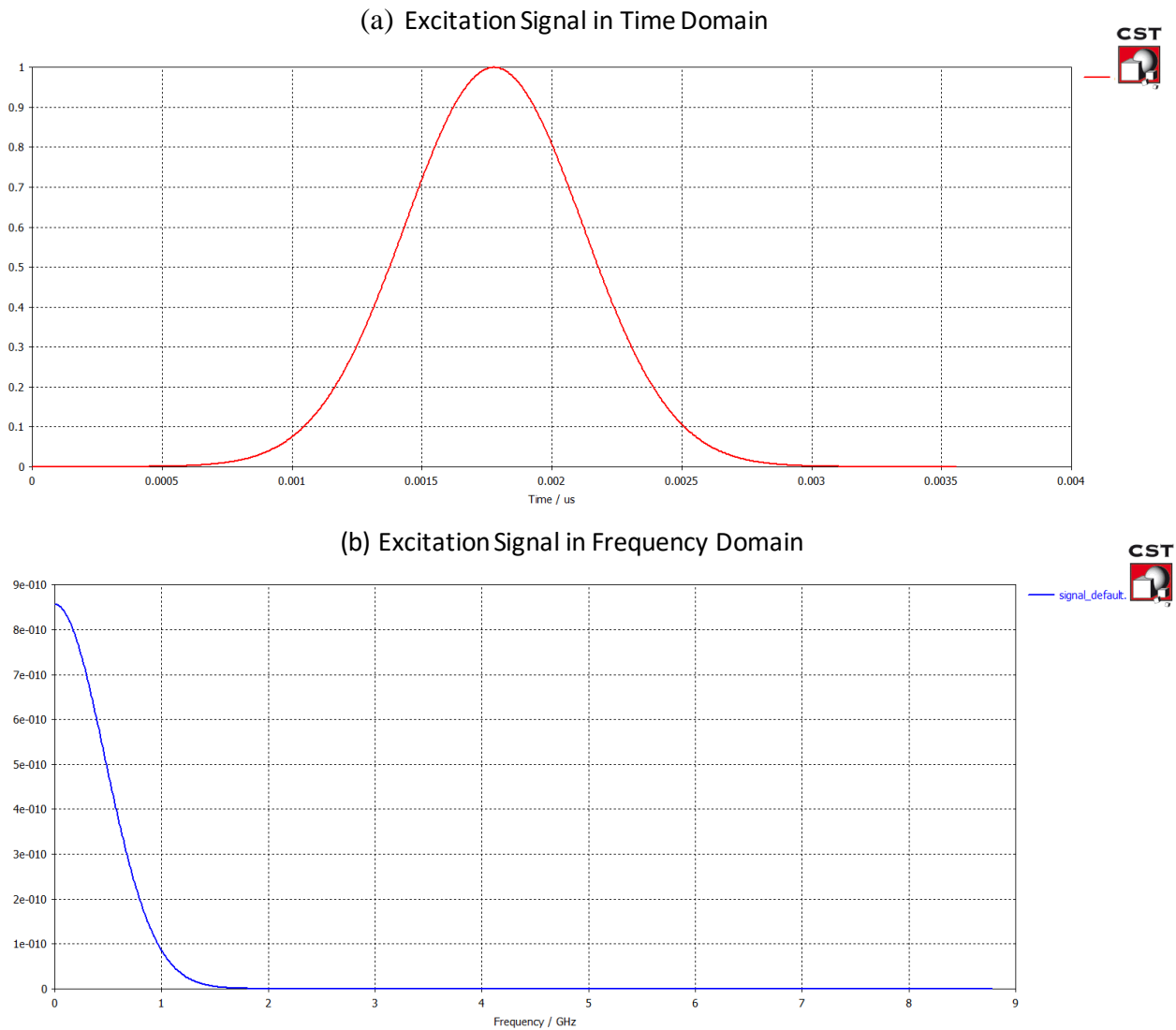
**Figure 11. Model Parameters**

“Open (add space)” was selected for the boundary condition since far field parameters were being measured. The symmetry of the samples was not considered so the symmetry planes were set to “none”. The boundary materials were set to normal or free space.

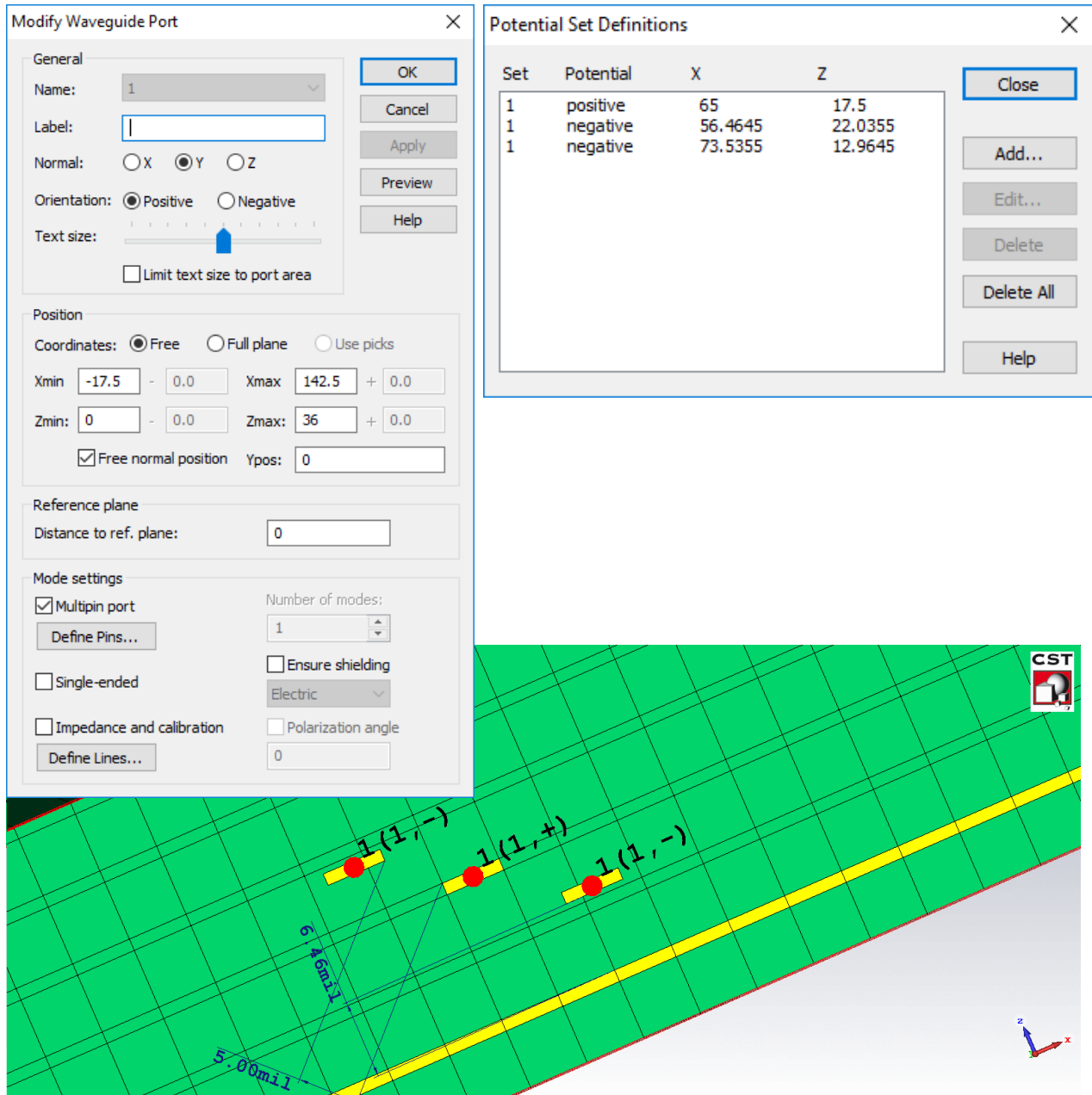
#### 5.1.3.1. Stimulus

In the actual implementation of the self-shielded designs, the current is split evenly between the split traces. In this case the current in the two return traces should be half the magnitude of the signal trace. The port settings don't seem to indicate how the excitation signal changes when two conductors are assigned the same name (see Figure 13). I set up current monitors on one of the samples to verify that the excitation in the split signals is representative of the actual implementation. The output of the current monitors validated that the return current is half the magnitude of the signal current, validating the excitation signal is representative of the expected use case. If this was not the case, the emitted field from the return would be twice as high and

would indicate a higher Gain in the simulation than would occur in actual use of the design. The excitation signal was a standard Gaussian pules. Figure 12 shows the excitation signal in the time domain and the frequency domain.



**Figure 12. Excitation Signal**



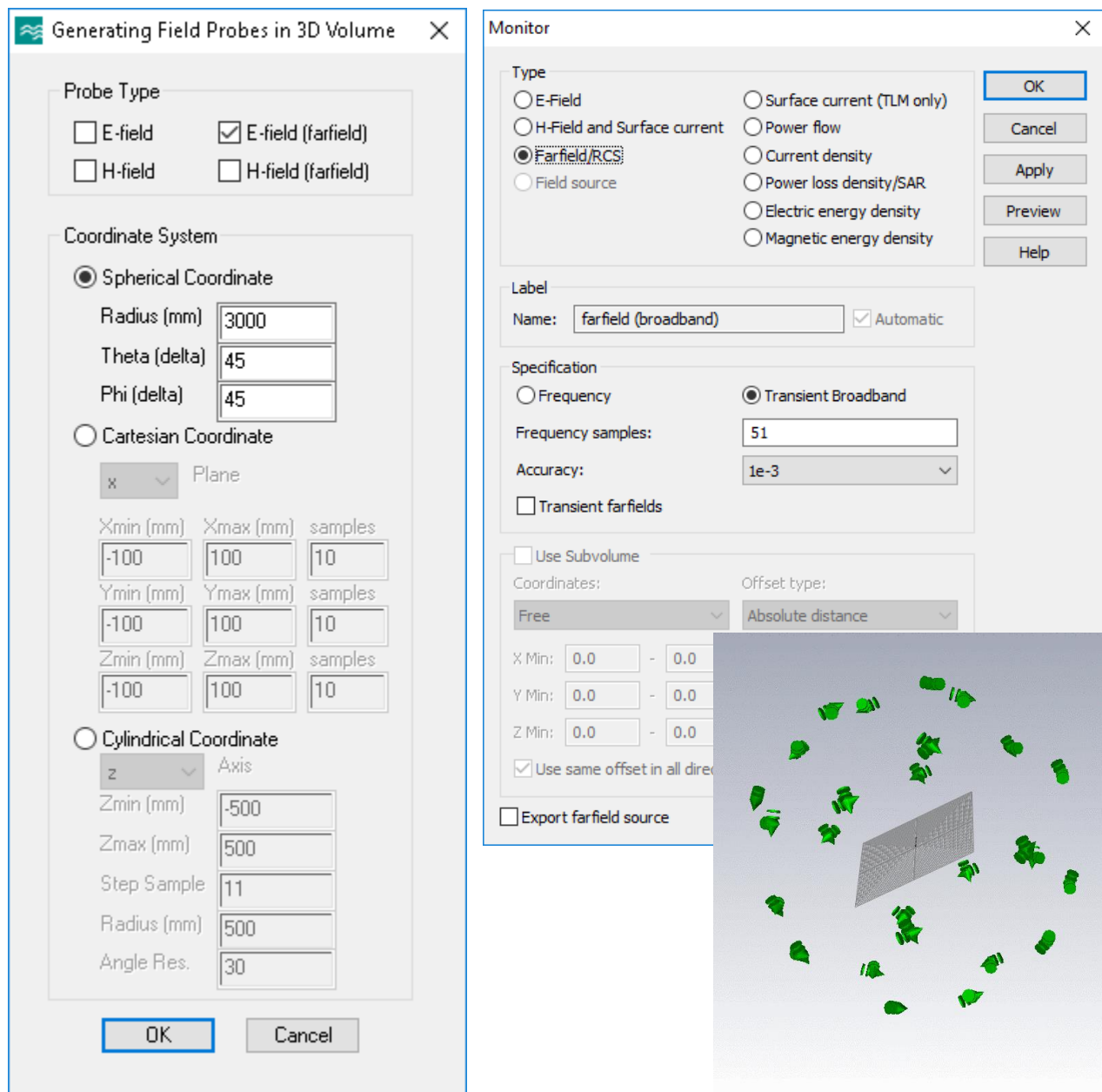
**Figure 13. Port Configuration**

Waveguide ports were used as opposed to discrete ports. In addition, the multipin option was used under mode settings. This allows the designer to configure the port to model differential signaling. The multipin setting was not used for sample A4 because it was modeling a single ended use case. The standard waveguide implementation was used for sample A4. The port modes and impedance verified that the Sample A4 model was in alignment with the expected use case.



### 5.1.3.2. Monitors/Probes

One of the EMC macros were used to set up far field probes spherically around the model (See figure 14).

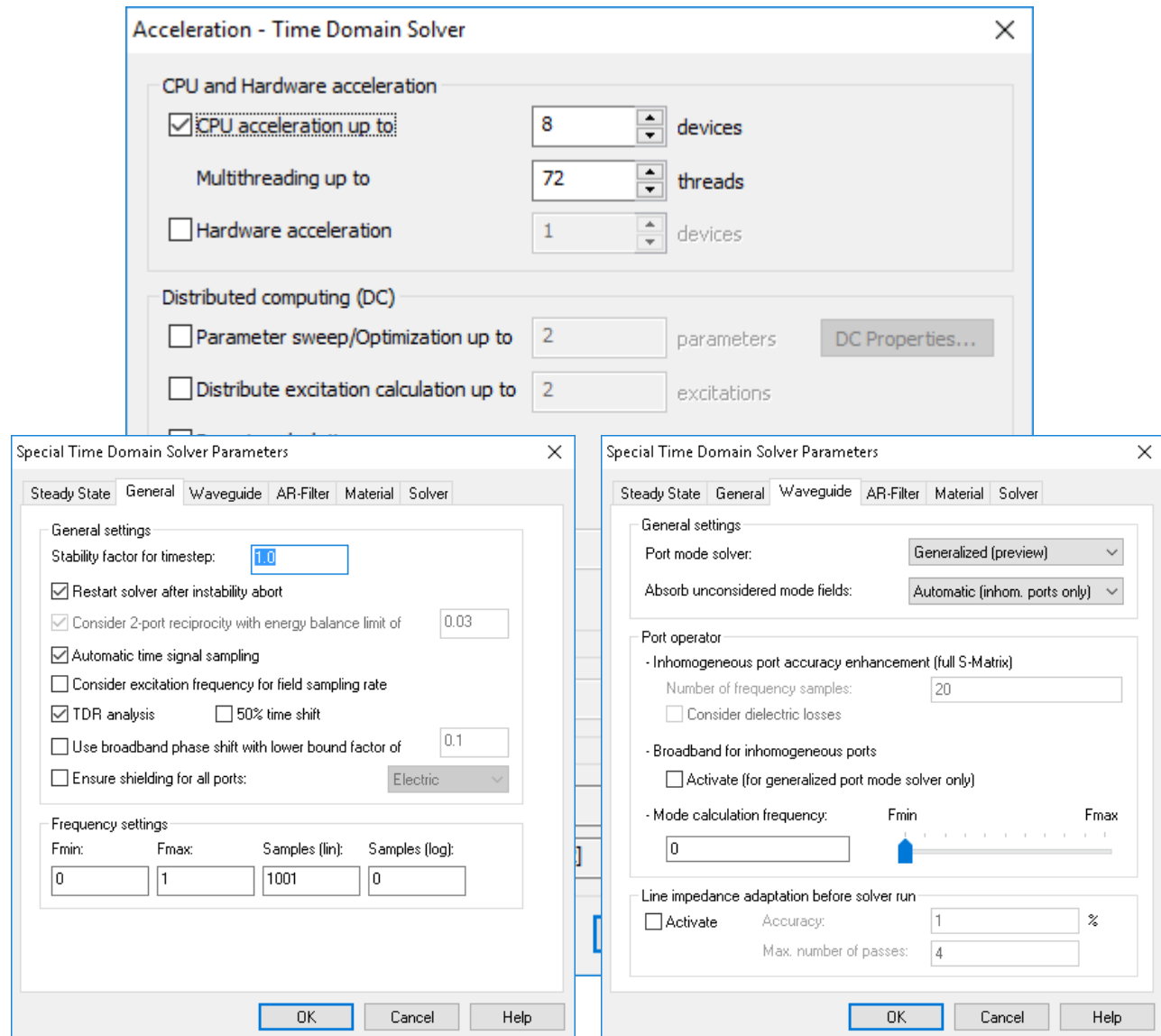


**Figure 14. Additional Probes and Monitors**

A Fairfield/RCS monitor with Transient Broadband was used to capture field strength vs frequency in the far field. Fifty-one frequency samples were used for a smoother trace. This monitor would produce good 1D radiation efficiency and gain plots making it easier to compare the design performances with these samples.

### 5.1.3.3. Solver

Please see figure 15 for solver Acceleration Settings and Solver Parameters. Solver parameters were configured based on CST support input to achieve the most accurate TRD measurements. TDR was turned on in the general tab. The port mode was changed to generalized, line “Impedance Adaptation Before Solver Run” was de-activated, and the Mode calculation frequency was set to 0 in the wave guide tab.



**Figure 15. Time Domain Solver Set Up**

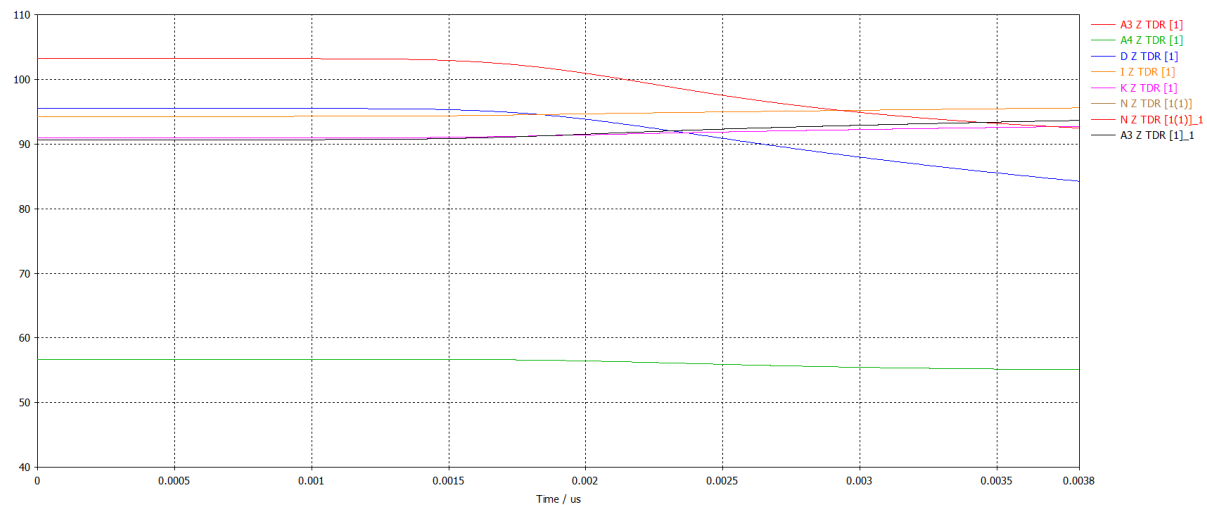
## 6. TEST/MODEL RESULTS

### 6.1. Simulation

#### 6.1.1. Impedance

The wave length is 0.3 meters given a dielectric constant of 2.9 at 1GHz. All these cables samples are 12K mils long or about 0.3048 meters long. The velocity of propagation is  $1.76 \times 10^8$ . This gives us an electrical length of 1.73 nm. If you consider the time that it takes for the signal to travel to the end of the cable and the reflections to return, the TDR electrical length should be  $3.52 \times 10^8$ . The fixed impedance samples must maintain a  $100 \pm 10$  Ohm differential impedance for all but one sample. Only one sample (A4) was single ended. Sample A4 was required to maintain  $50 \pm 10$  Ohms (Fleisch 124).

(a) Fixed Impedance TDR traces



(b) Fixed Area TDR trace

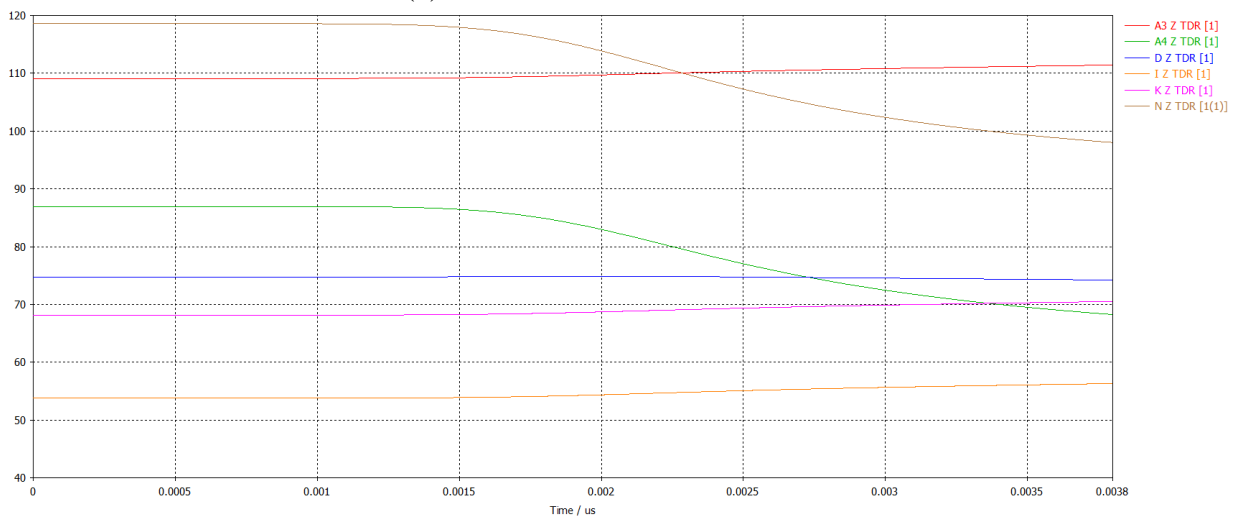


Figure 16. TDR Traces of All Samples

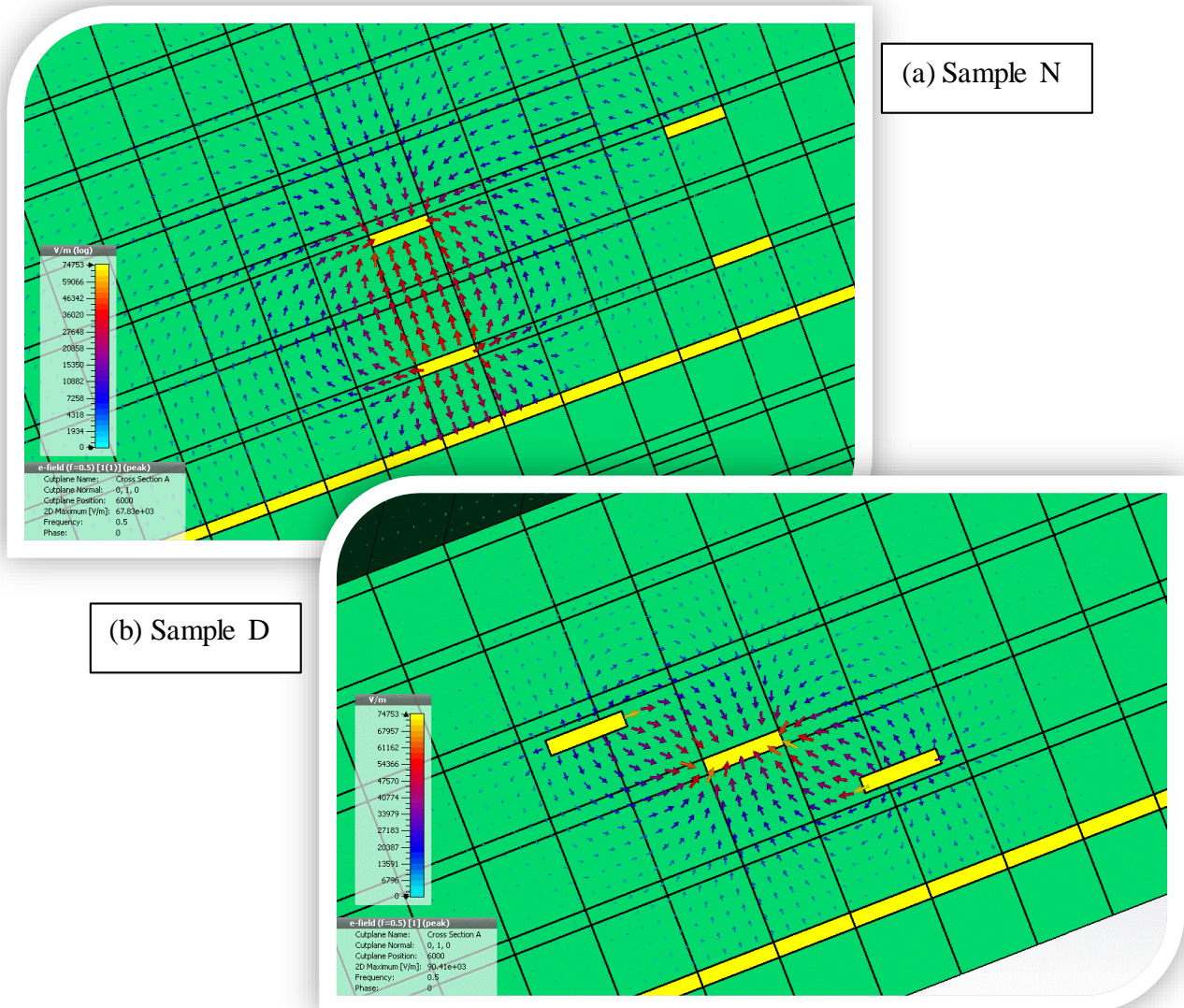
## 6.1.1.1. Fixed Area

## 6.1.1.2. Accuracy in question

The accuracy of the model came into question based on TDR observations. Several mesh refinement approaches were taken to remove the anomaly. Based on CST support feedback, TDR is more sensitive to less than ideal mesh's. If dx, dy, or dz of the mesh cells are far from equal it can cause a buildup of error in the coarser direction. In this case the coarser direction was along the length of the cable. This could add error to the TDR. Unfortunately, this could not be rectified without creating tens of millions of mesh cells and making the simulation too large to solve considering the number of runs required. On the other hand, Gain and radiation efficiency is calculated from emissions in all directions. It is reasonable to assume that the most important parameters were not as sensitive as the TDR in these models. To test this assumption, I tested the sensitivity of Efficiency and Gain to changes in the mesh. I ran three different mesh's starting from the mesh refinement used for all the samples, then doubling the number of cells per wavelength for the second simulation, and finally tripling the number of mesh cells for the third simulation. Doubling and tripling cells would only impact the cell dimensions in the lengthwise direction because the local mesh properties controlled the mesh cells in the other directions. This process would allow me to observe Gain and efficiency change as the number and dimensions of the mesh cells change. Finally, I ran the model using adaptive mesh. The Efficiency was -55dB on the first run, -57dB on the second, and back to -55dB on the third run. Resulting in a  $\pm 2\%$  variation. The Efficiency finished the adaptive meshing after the minimum 2 runs because it met the 2% requirement. An accuracy of 2% is acceptable for this project.

### 6.1.2. E and H field observation

The self-shielding works by creating tighter field coupling. The tighter coupling can be seen visually between the best performing self-shielded cable and one of the worst performing cable.



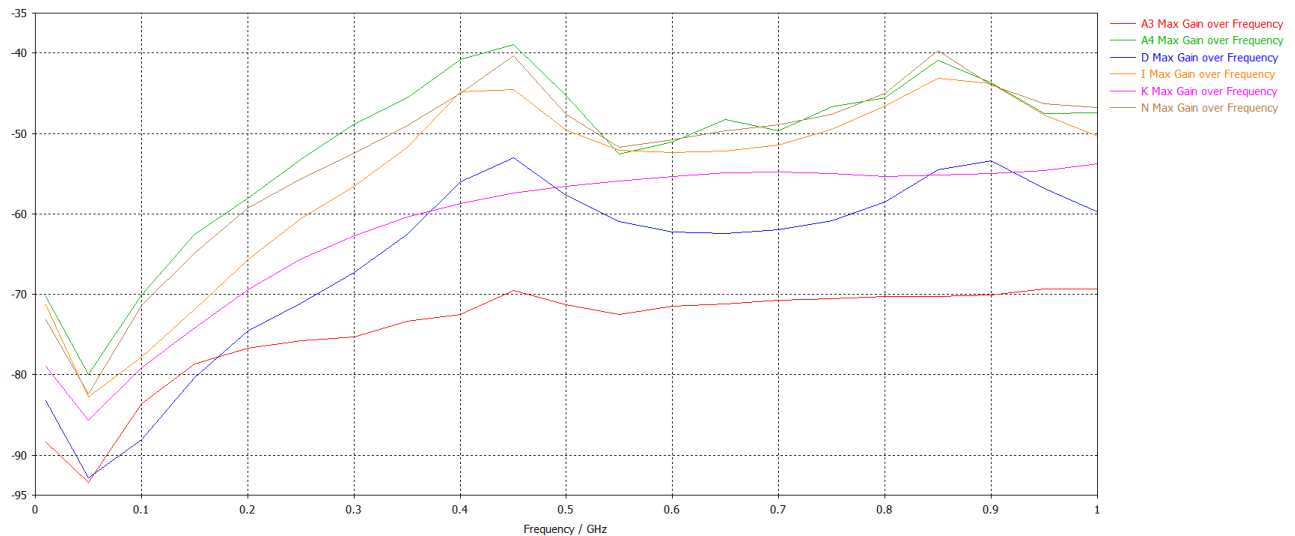
**Figure 17. Samples N and D E-fields at 0.5 GHz**

### 6.1.3. Gain

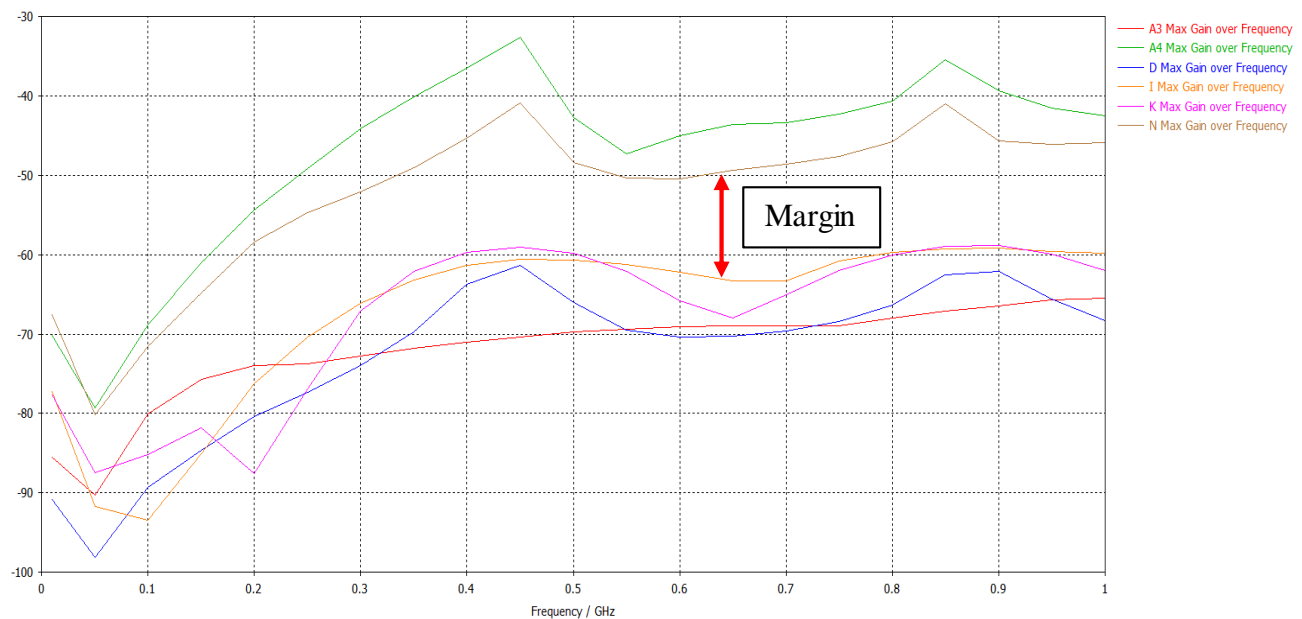
The lowest Gain will be the more favorable result when evaluating the Gain performance on these samples. The best performing design is one of the standard designs (A3 sample). This is probably because of its proximity and orientation to the ground plain. Further evaluation will be required to understand why this sampler performed so well. The other two standard designs were the worst performing samples. The best performing self-shielded cable is between sample K and D. Sample D performs better on average but displays some resonance at 450MHz and 900MHz where it displays enhanced gain. Finally, the worst performing sample is the standard single

ended sample and sample N. In general, the self-shielded designs perform the best. The margin (figure 18 (b)) between the performance of the standard samples and the self-shielded sample shrink when impedance control is required. The improved shielding performance may not be worth the trade in space given the increase in cross sectional area for the implementation of the self-shielded samples. On the other hand, the self-shielded designs are a better option if impedance control is not required or can be implement at lower impedance across the entire system or subsystem. This can be the case if all the transmission lines are all contained in one board and only your inputs and outputs need to be matched to standard impedances. (Poza 274)

(a) Fixed Impedance Gain



(b) Fixed Area Gain

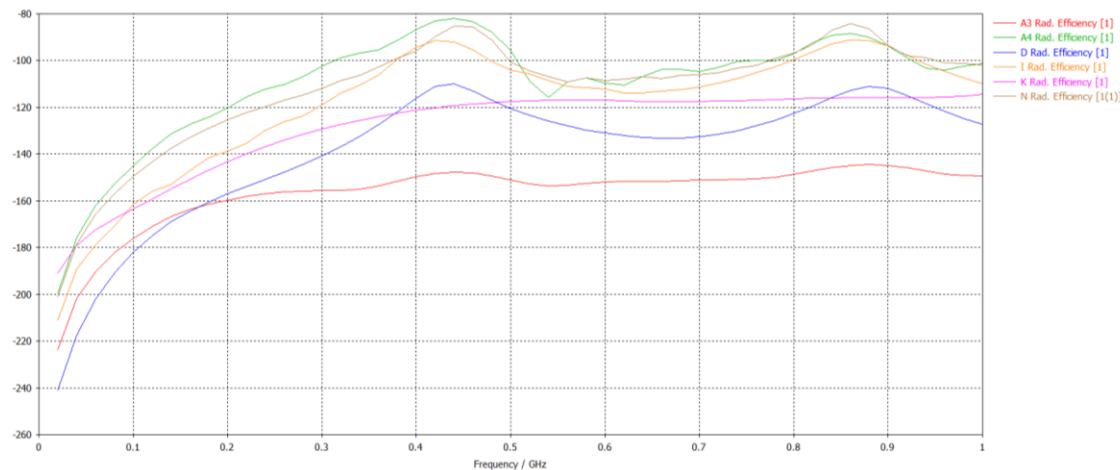


**Figure 18. Gain of All Samples**

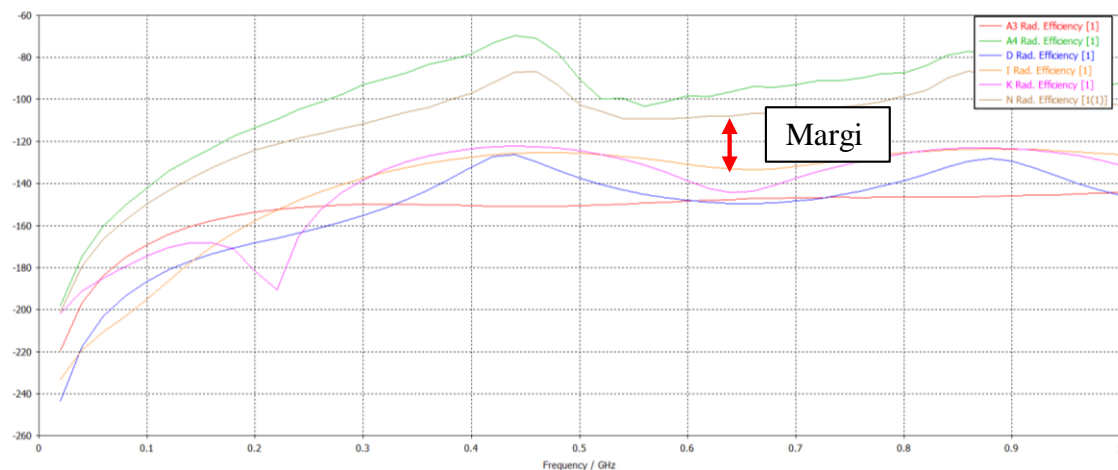
#### 6.1.4. Efficiency

The Antenna Radiation Efficiency is also known as the conduction-dielectric efficiency ( $e_{cd}$ ). Its defined as the power delivered to the Radiation resistance divided by power delivered to the sum of the Radiation Resistance  $R_r$  and the conduction dielectric resistance  $R_L$ . Another helpful representation of the Radiation Efficiency ( $e_{cd}$ ) is  $e_{cd} = P_{rad}/P_{in}$ . The lowest  $e_{cd}$  will be the more favorable result when evaluating the  $e_{cd}$  performance on these samples. The best performing design for efficiency is the A3 sample. The explanation given in section 7.1.3 is applicable for efficiency as well. The best performing self-shielded cable is between sample K and D. Sample D performs better on average but displays some resonance at 450MHz and 900MHz where it displays enhanced gain. Finally, the worst performing sample is the standard single ended sample and the N sample. In general, the self-shielded designs perform the best. Figure 19 displays  $e_{cd}$  in dB while Figure 20 displays  $e_{cd}$  in linear magnitude. (Balanis 110)

(a) Fixed Impedance ( $e_{cd}$ )

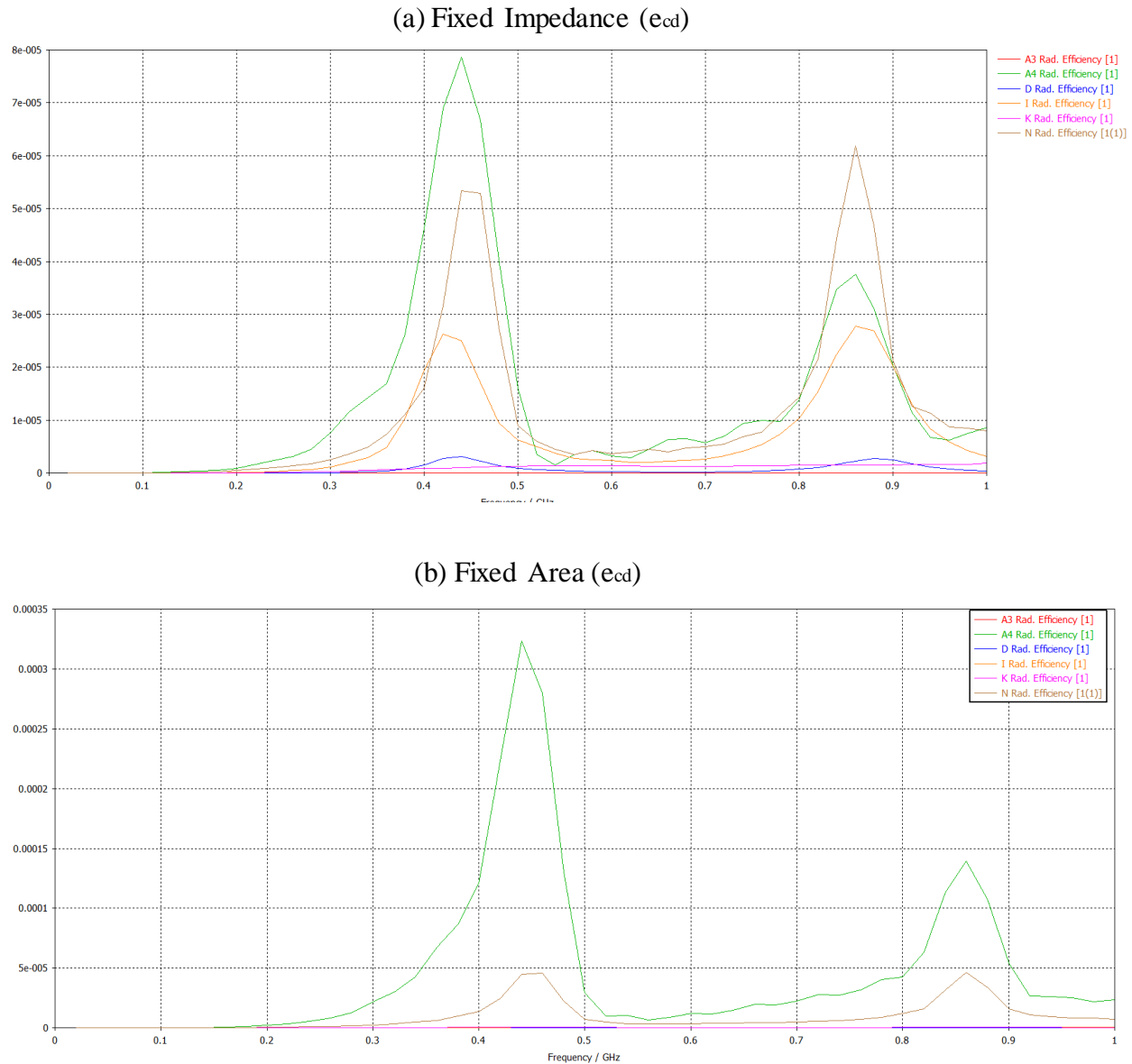


(b) Fixed Area ( $e_{cd}$ )





**Figure 19. Radiation Efficiency in dB**



**Figure 20. Radiation Efficiency in Linear Magnitude**

## 6.2. Conclusion

In conclusion, the self-shielded samples do perform better in regards to EMC by several dB on average compared to the standard samples. When loop area is fixed, the performance difference is in the tens of dB on average. The improved EMC performance is reduced when required to match impedance at 100 ohms or 50 ohms single ended. The reason for the improved EMC performance is tighter field coupling between traces. It is noted that there are other design features that can increase field coupling. Generally, anything that increases capacitance will increase field coupling and reduce loop impedance which isn't a new concept to transmission



line design. You can do this by increasing surface area of the traces. You can also make the outside traces wider than the inside trace when you are splitting the return or negative signal. Lowering the dielectric content helps to mitigate the sharp drop in impedance without needing to spread out the traces as much.

## 7. BIBLIOGRAPHY

Balanis, Constantine A. *Antenna Theory - Analysis and Design (3rd Edition)*. John Wiley & Sons. Print.

Fleisch, Daniel A. *A Student's Guide to Maxwell's Equations*. Cambridge: Cambridge UP, 2014. Print.

Pozar, David M. *Microwave Engineering*. Hoboken, NJ: Wiley, 2012. Print.

Doren, Tom Van, Dr. "Grounding and Shielding of Electronic Systems." EMC Class. NM, Albuquerque. 26 Apr. 2016. Lecture.

Ott, Henry W. *Noise Reduction Techniques in Electronic Systems*. 2nd ed. New York: Wiley, 1988. Print.

Sandia National Laboratories is a multi-mission laboratory managed and operated by Sandia Corporation, a wholly owned subsidiary of Lockheed Martin Corporation, for the U.S. Department of Energy's National Nuclear Security Administration under contract DE-AC04-94AL85000.